Lecture 2 . Structures at large scales:

Clusters/Superclusters- filaments and beyond

I A T E
CONICET
U N C
OAC

Diego Garcia Lambas, IATE - Observatorio Astrónomico. Córdoba Argentina.

Espirito Santo, September 2022

- The largest scales structures are manifest in the CMB fluctuations.

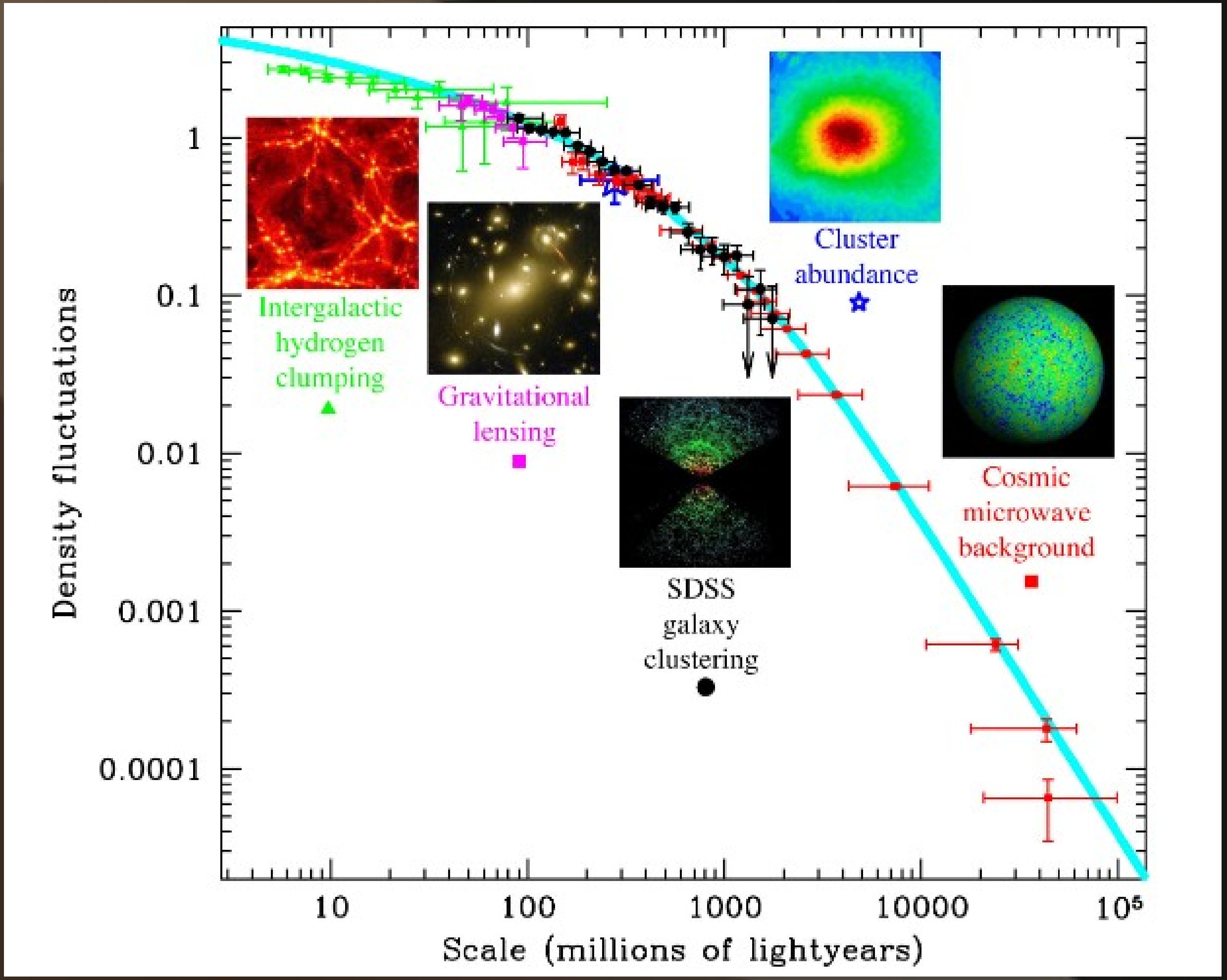

Inhomogeneous universe

- Initial conditions imprinted in the CMB
- WMAP, Planck, + new experiments on the way

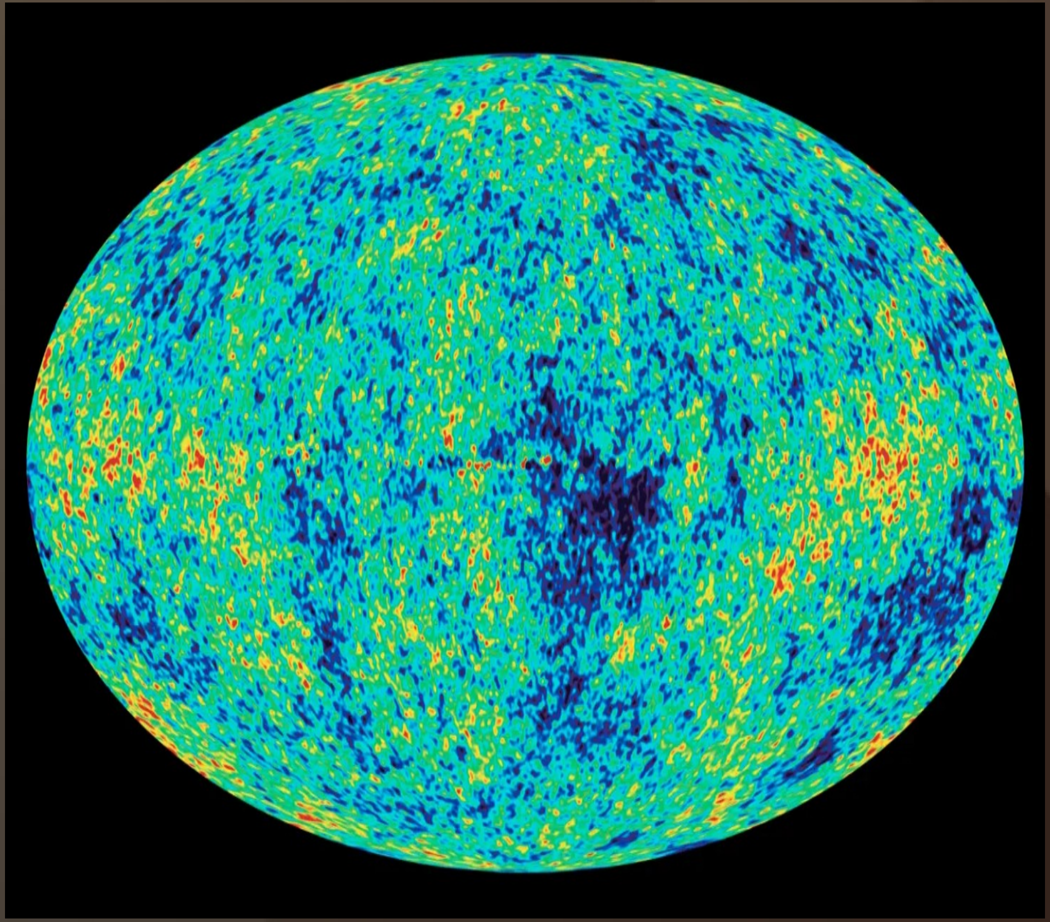

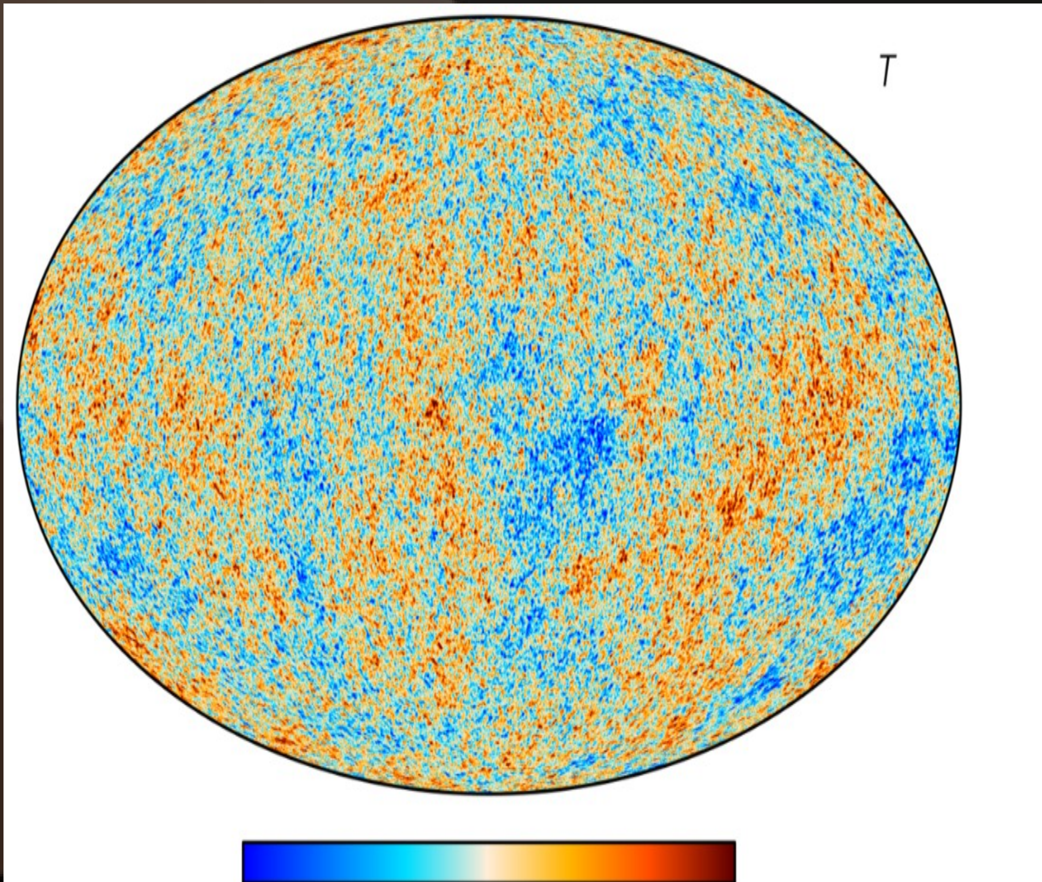

Observed temperature spectrum → primordial fluctuations + global effects (transfer function)

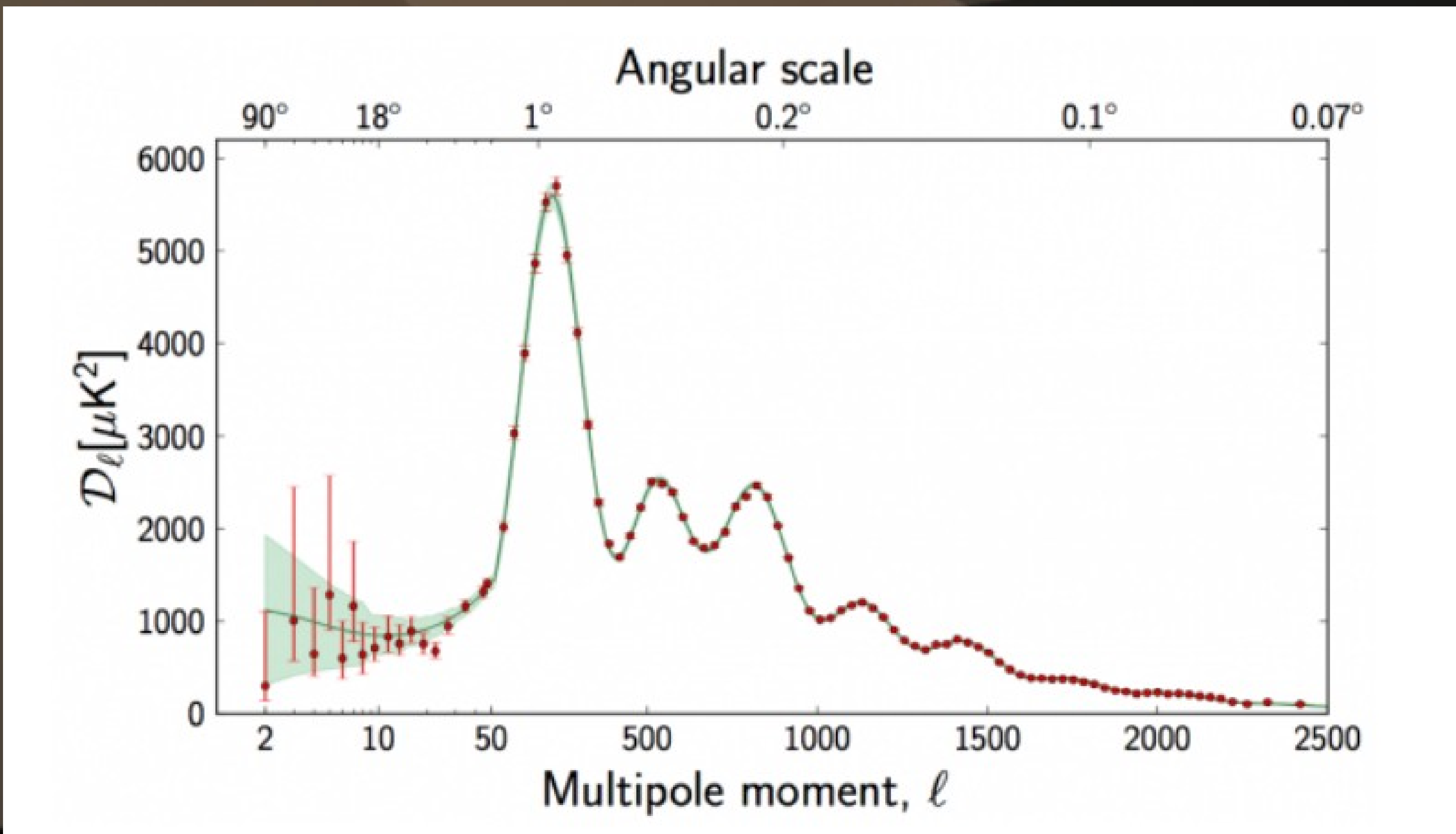

CMB studies can also shed light on astrohpysics of the intergalactic medium and lensing by structure

CMB-structures interaction provide probes of the distribution of mater.

→ Cosmological tests.

Direct observation of dark matter not observed, yet

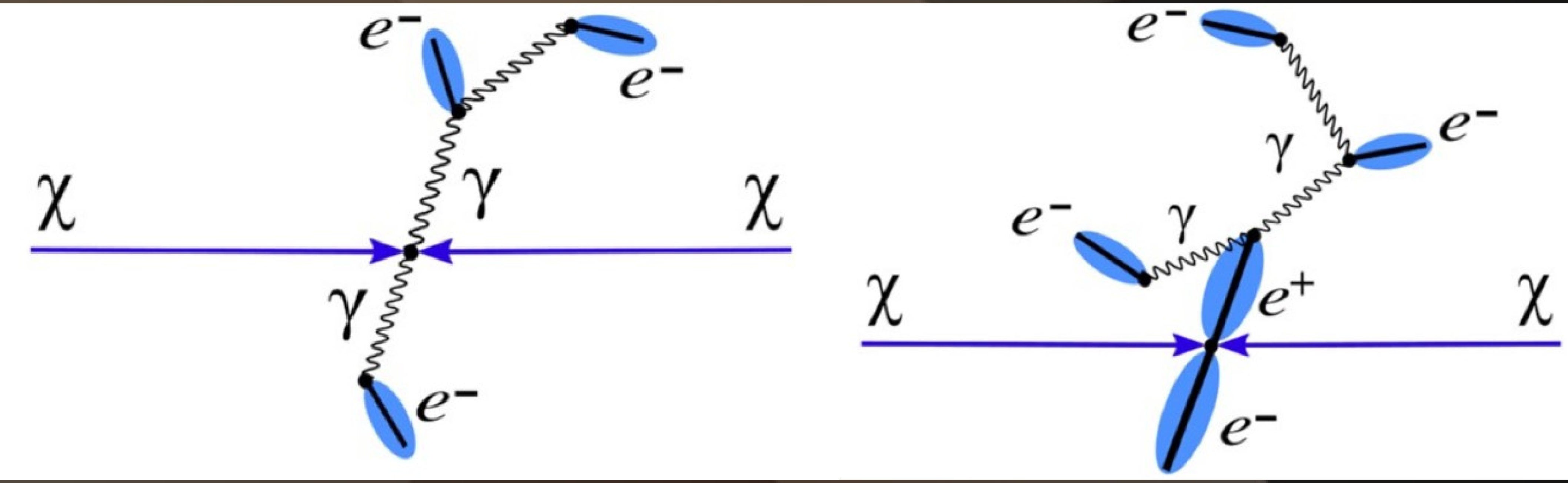

- For this reason every constrain from galaxies and structure is of crucial mportance.

Clusters, cross-roads in structure

Anisotropy modelling, for WL cluster halos E. Gonzalez et al. 20,21,22

- In both simulations and data

$$\epsilon := (1 - q)/(1 + q$$

$$\Sigma(R) = \Sigma(r,\theta) := \Sigma_0(r) + \epsilon\Sigma_2(r)\cos(2\theta),$$

Shapes, alignment wrt BCG, galaxies and ICL

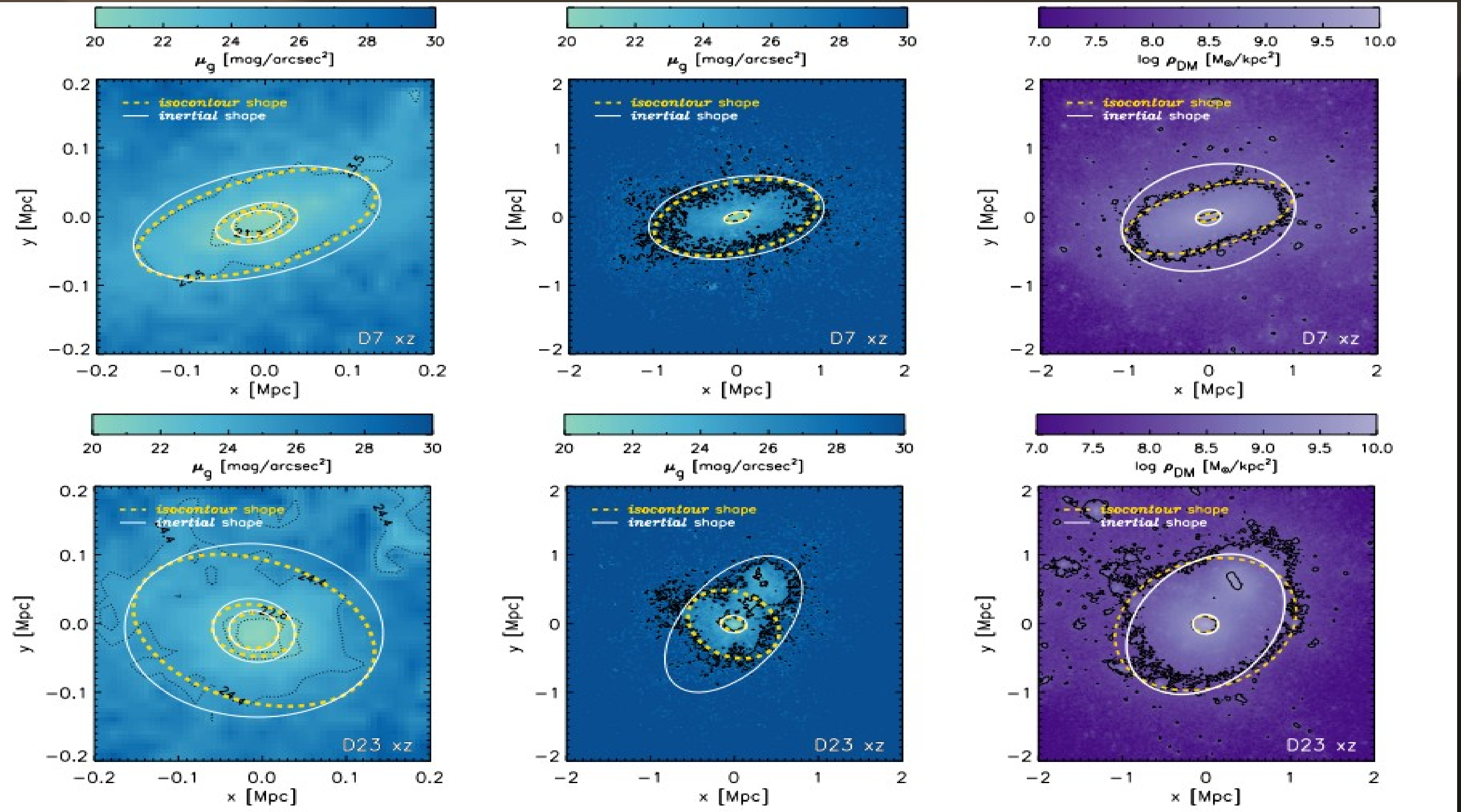

Figure 3. A schematic view of the shape and orientation angle determinations for an early and late formed cluster is presented in the top and bottom panels, respectively. Left and middle panels show the surface brightness maps of the BCG and the BCG+ICL, respectively. The right panels depicts instead the DM density distribution. In all the panels solid line ellipse parameters are obtained from the shape tensor selecting stars or DM particles, as the case may be, within different radii. Dashed line ellipses are instead the best fits returned by the rutine ELLIPSE for the same radii. The corresponding isophotes or isodensity contours are also shown in black. In the case of the BCG we show elipses with SMAs of 30kpc (internal), 50kpc (middle) and $0.1R_{500}$ (external). In the cluster scale we depict $0.1R_{500}$ (internal) and R_{1000} (external). Notice however that in the case of the ICL for the late-formed cluster (middle bottom) the *isocontour* shape determination does not reach up to R_{1000}, the proximity of a merging halo is apparent.

Simulations show that galaxies are more elongated than DM.
ICL, (galaxies) and DM well aligned within 5 (10) deg.

Results for redMaPPer clusters

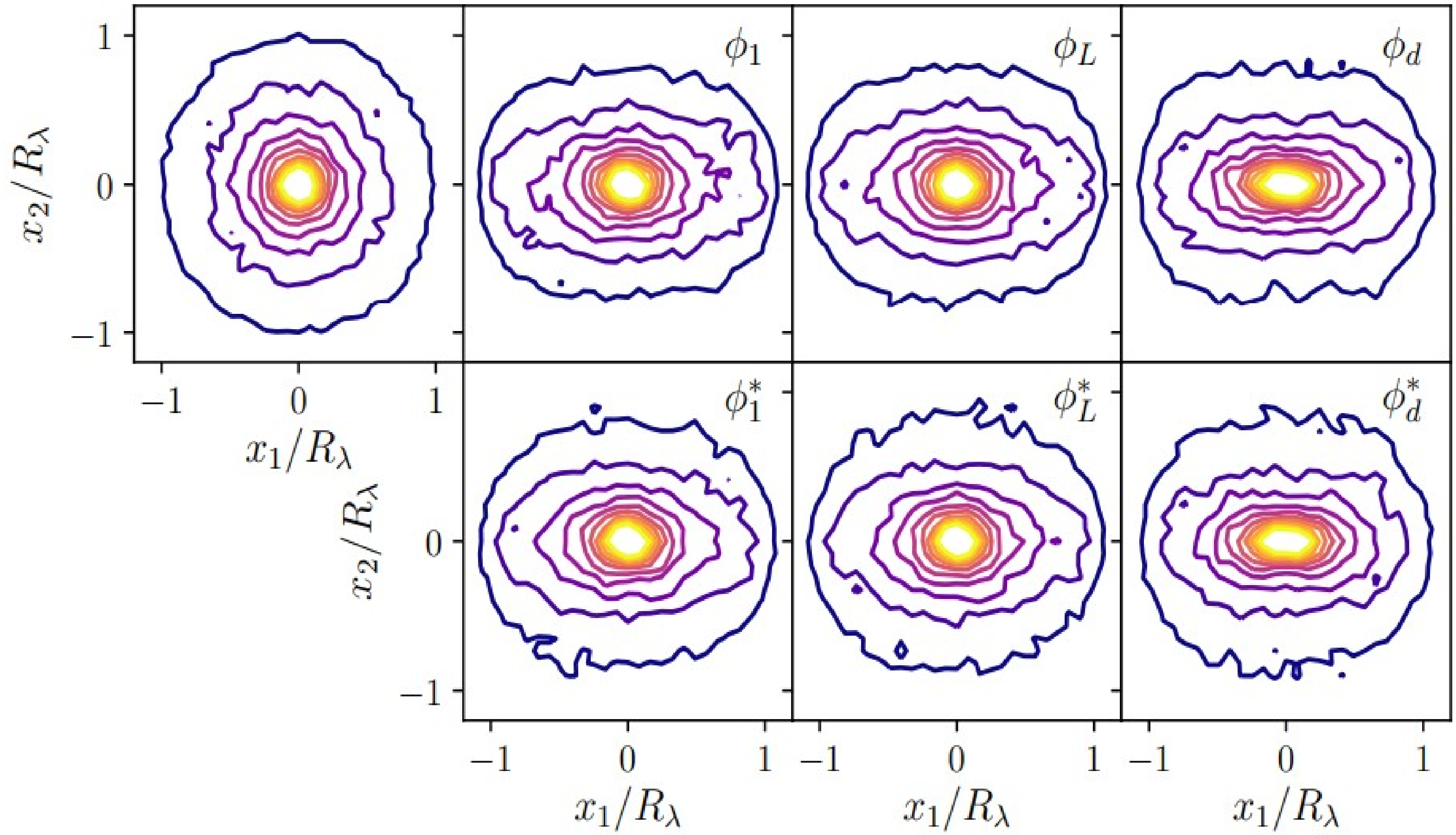

Figure 2. Satellite number density contours for the sample of redMaPPer clusters used in this work, obtained by stacking the galaxies aligned according to the estimated orientation angle. Projected positions, x_1 and x_2, are re-scaled with the cluster radius, R_λ. The first panel at the left was obtained without aligning the clusters. First row of panels is obtained considering all the satellites in the catalogue and the second row discarding the galaxies with $p_{mem} < 0.5$ to estimate the orientation angle. Second, third and fourth columns correspond to the orientation computed considering a uniform, a luminosity and a distance weight to compute the quadrupole moments, respectively.

Robust results for e ~ 0.2

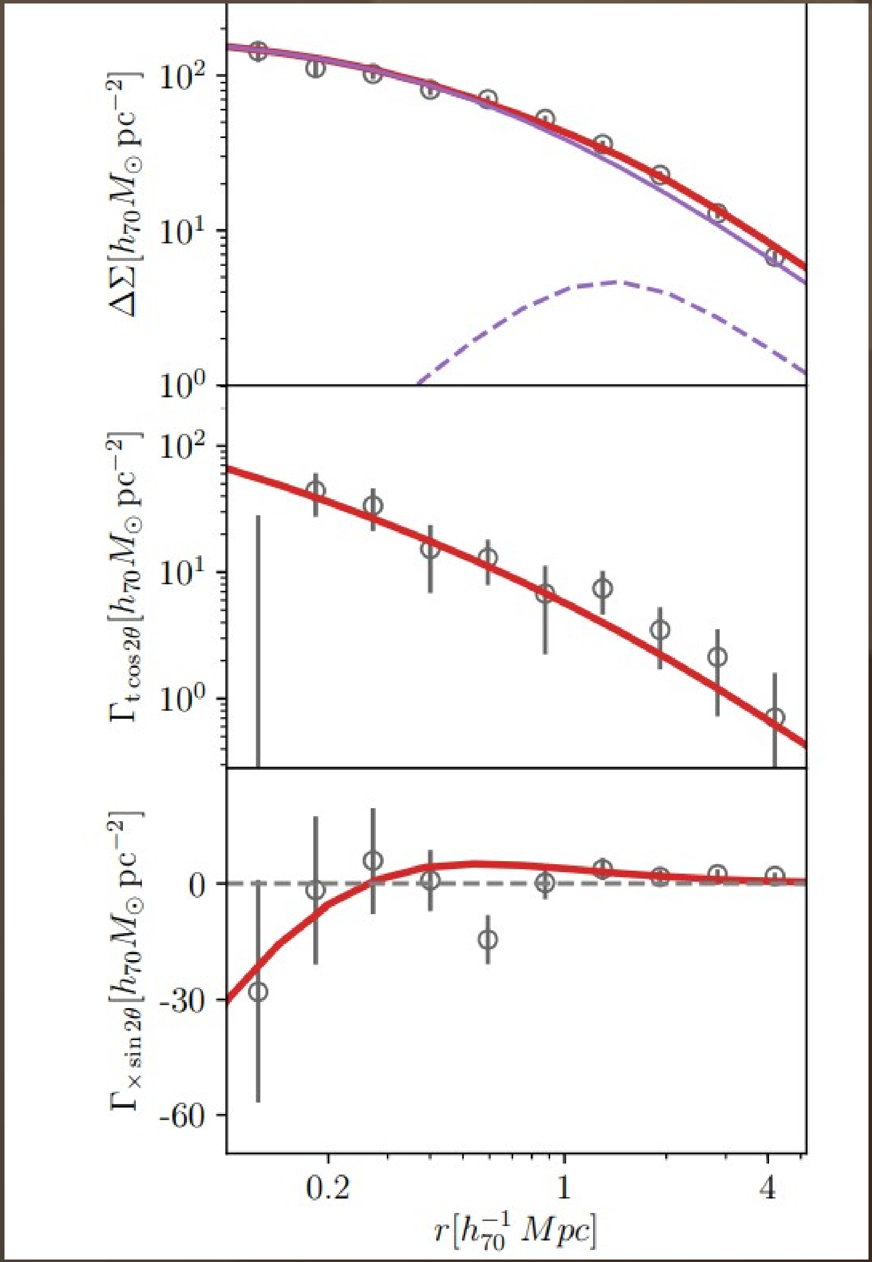

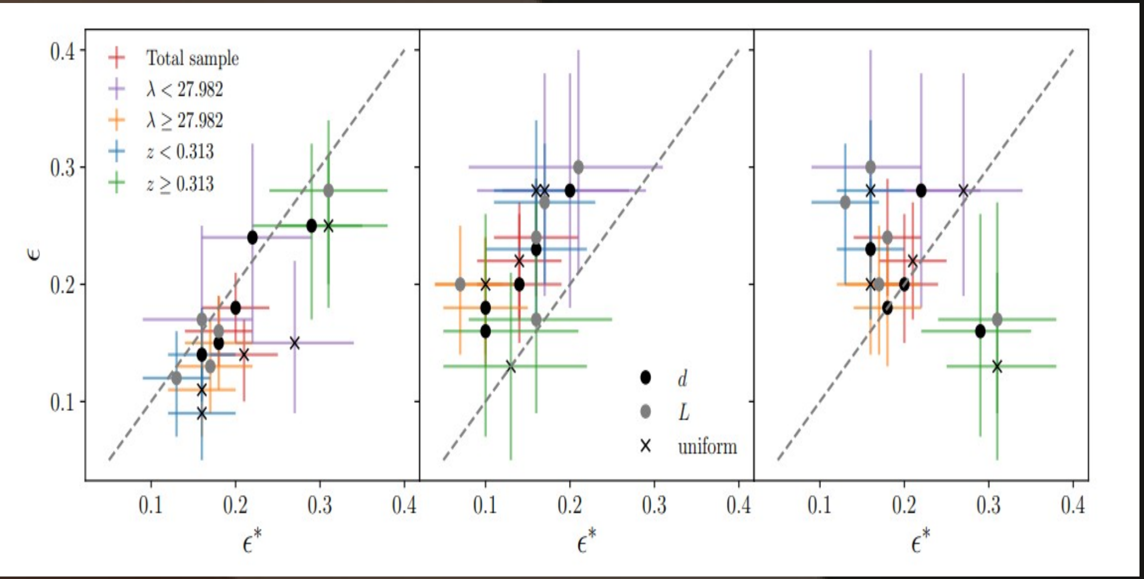

Clusters of galaxies as cosmic probes

- Cluster abundance
- Cluster charateristics and dynamics

Phase space of clusters under different models of self interacting dark matter

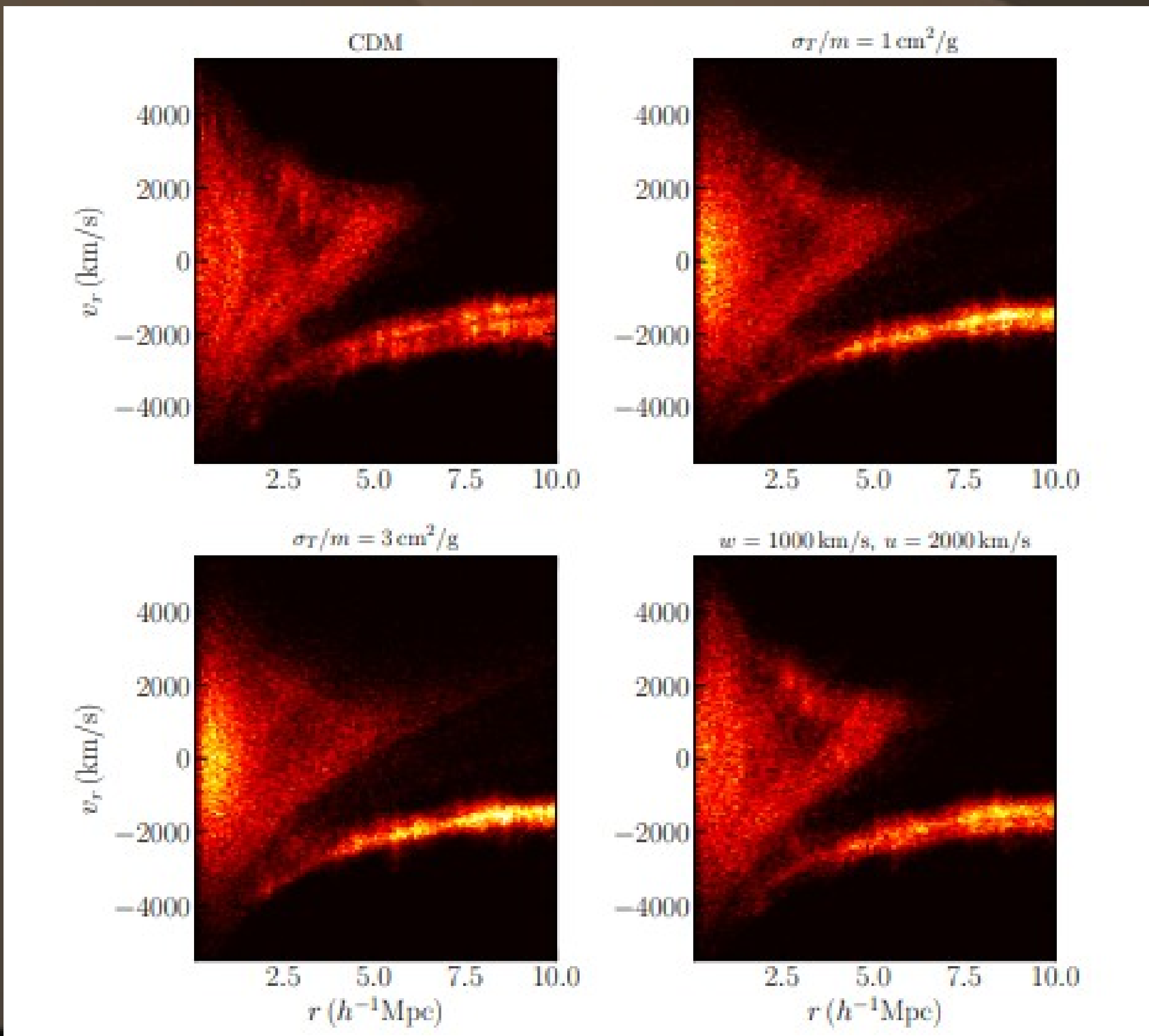

- Benarjee et al. 2020

Cluster dynamical state and mass function

Seppi et al. 2021.

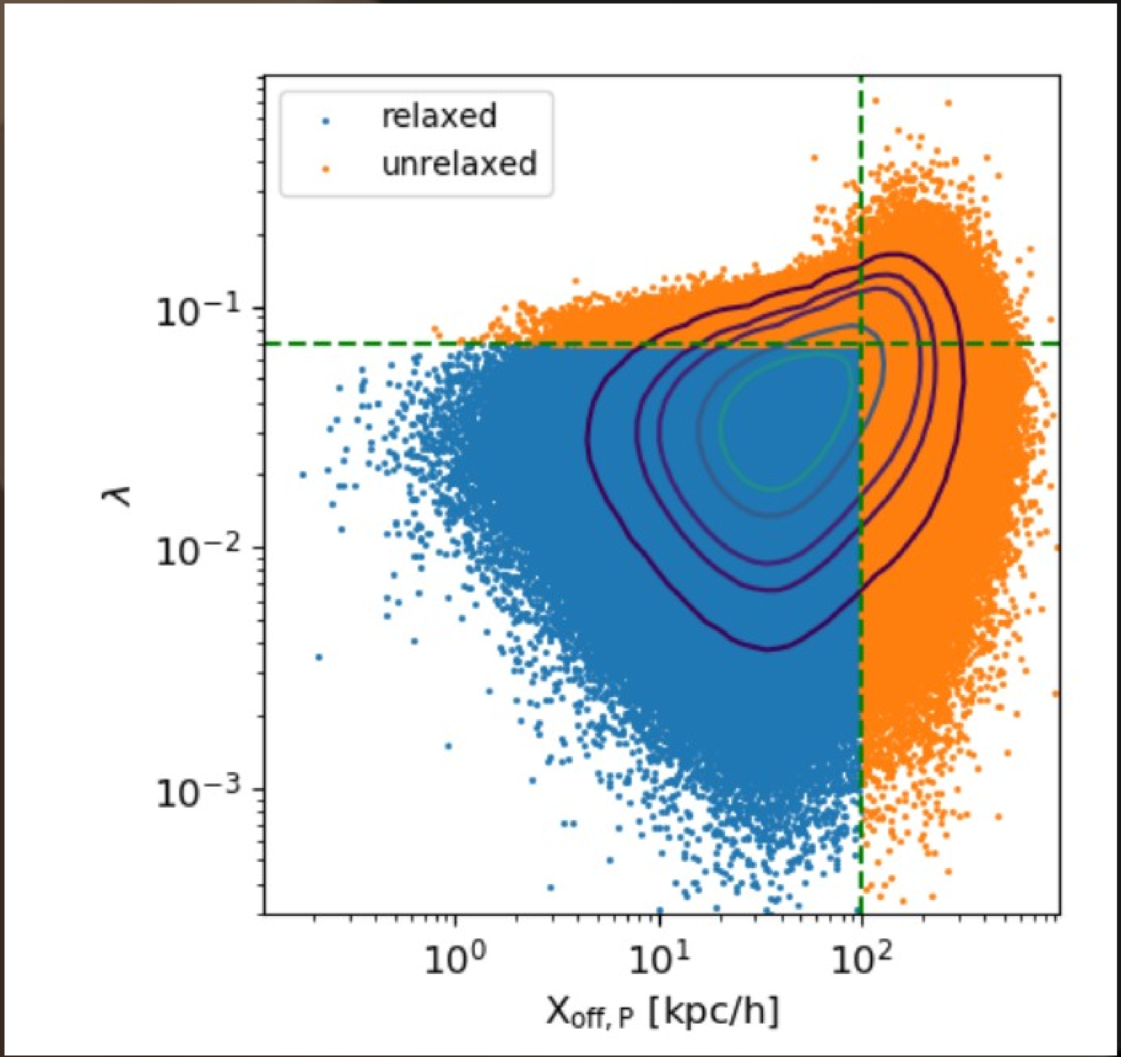

- **Structure coherence → alignments**

BCG and cluster alignment, a primordial or an evolutionary effect?

Raggone et al.
2020

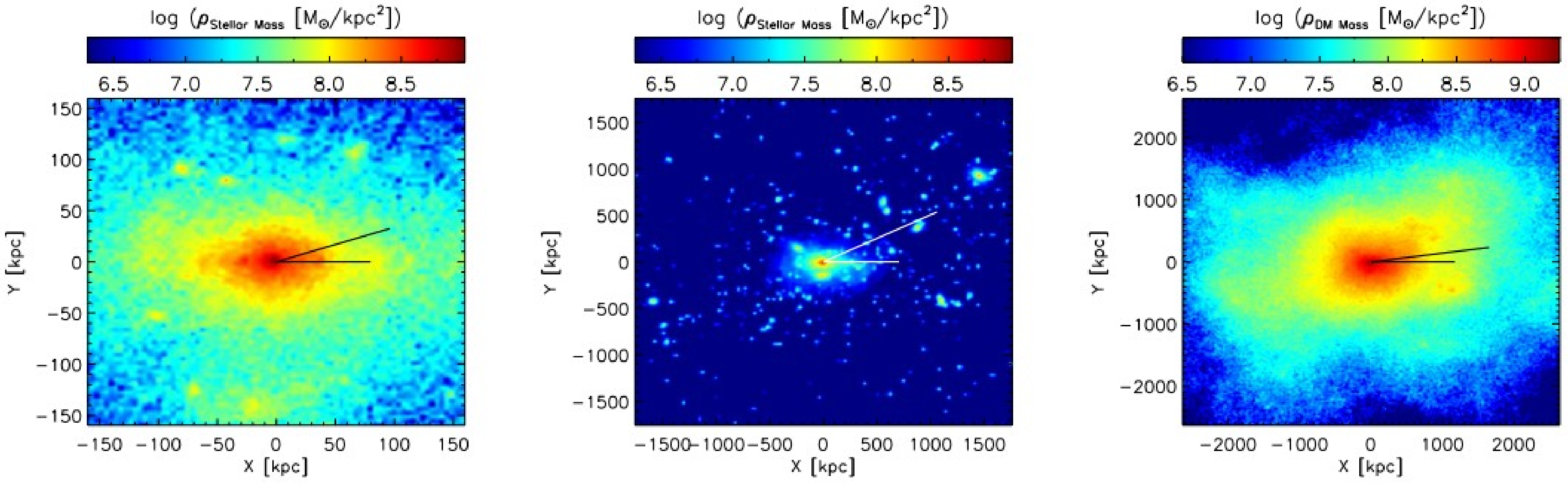

Figure 1. An example of the different mass distributions and their elongation axis for one of our simulated clusters at $z = 0$. Left Panel: BCG stellar mass distribution. The short line corresponds to the BCG elongation axis, this is set to coincide with the x-axis in all panels. The long line marks instead the cluster galaxies elongation axis. Middle Panel: satellite galaxies distribution, short and long lines are as in the left panel. Right panel: cluster DM distribution. The long line follows the direction of the cluster DM elongation axis.

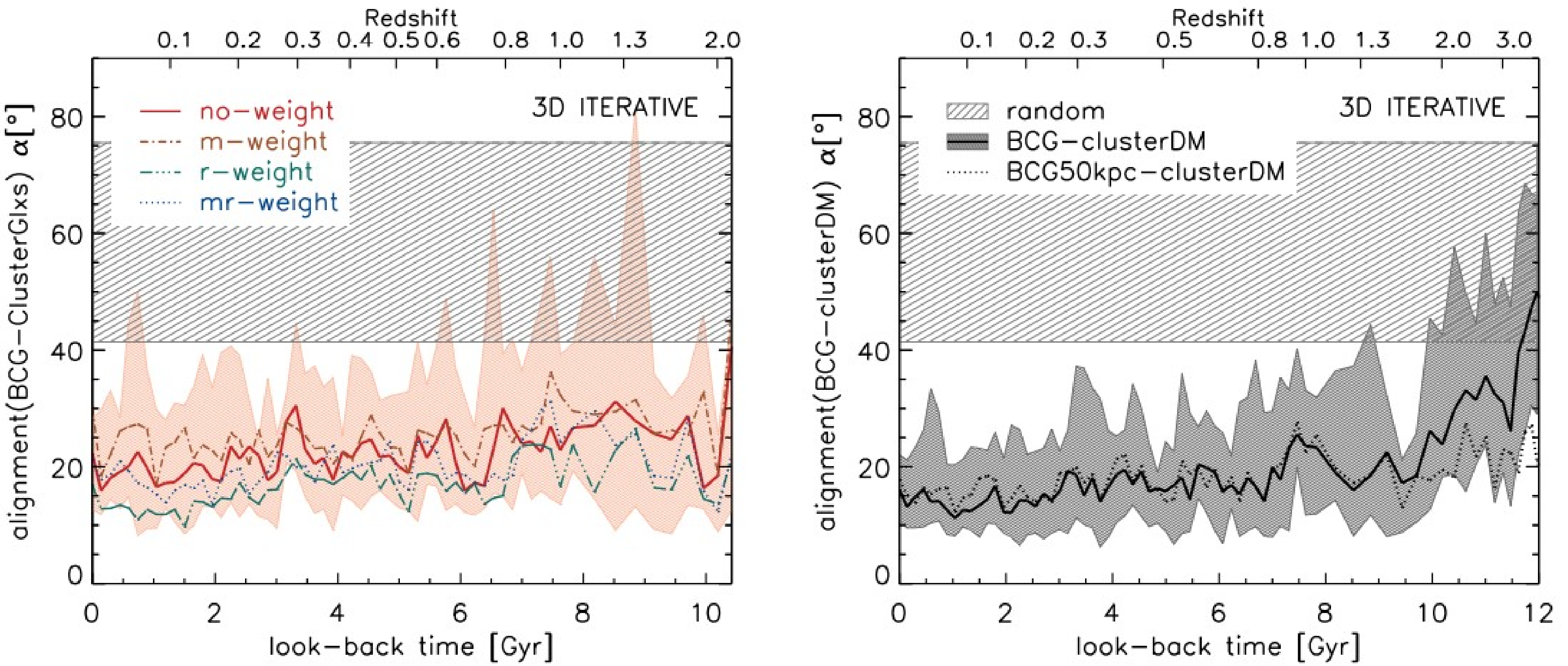

Figure 2. Median values of BCG-ClusterGlxs (left panel) and BCG-ClusterDM (right panel) alignment angles for our set of 29 simulated cluster at each epoch (note that limits in the x-axis are different in both panels, see text). The shaded area encloses the 25%-75% percentiles of the distributions. For sake of clarity in the left panel only the no-weight case percentiles are shown. Up to $z \lesssim 2$ there is no clear evolution of the alignment. At $z \gtrsim 2$ the BCG-ClusterDM alignment angle increases gradually toward earlier epochs, nevertheless this is not the case if BCG is defined as stars particles inside a 50kpc fixed aperture (dotted line). The horizontal dashed area corresponds to the 25%-75% percentiles of the angle distribution for random directions in 3D (see text).

Our neibourhood: Lainakea Supercluster

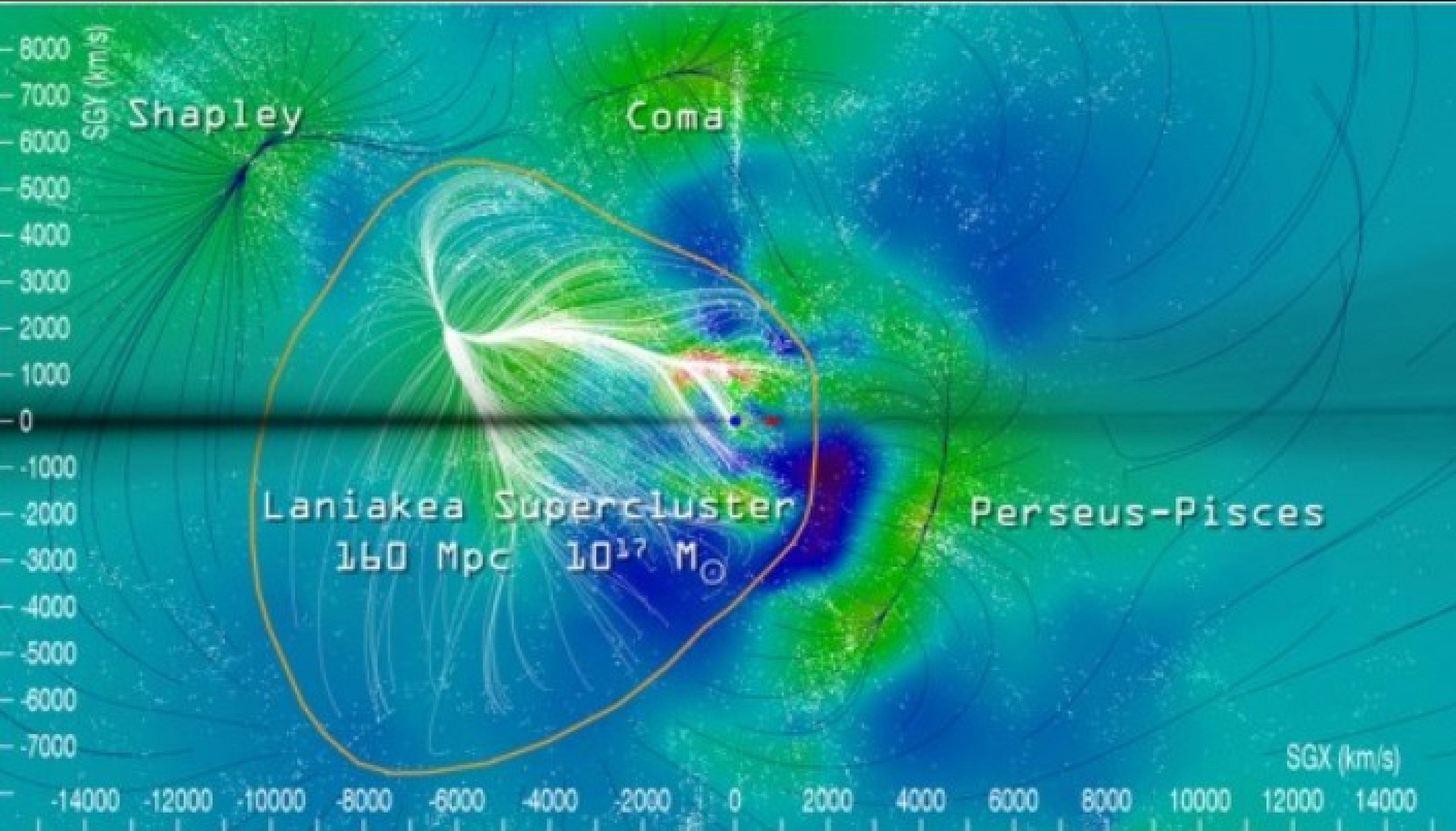

Superstructures in the universe FVS

In LCDM, a spherical shell enclosing at least 7.88 of the present-day mean mass density will evolve into a virialized structure in the distant future, Dunner et al. 2012.

$$\frac{\bar{\rho}^{mass}_{shell}}{\bar{\rho}^{mass}_{bck}} = 7.88$$

FVS provide a natural definition of superstructures in the universe

Luparello et al.2013-2014

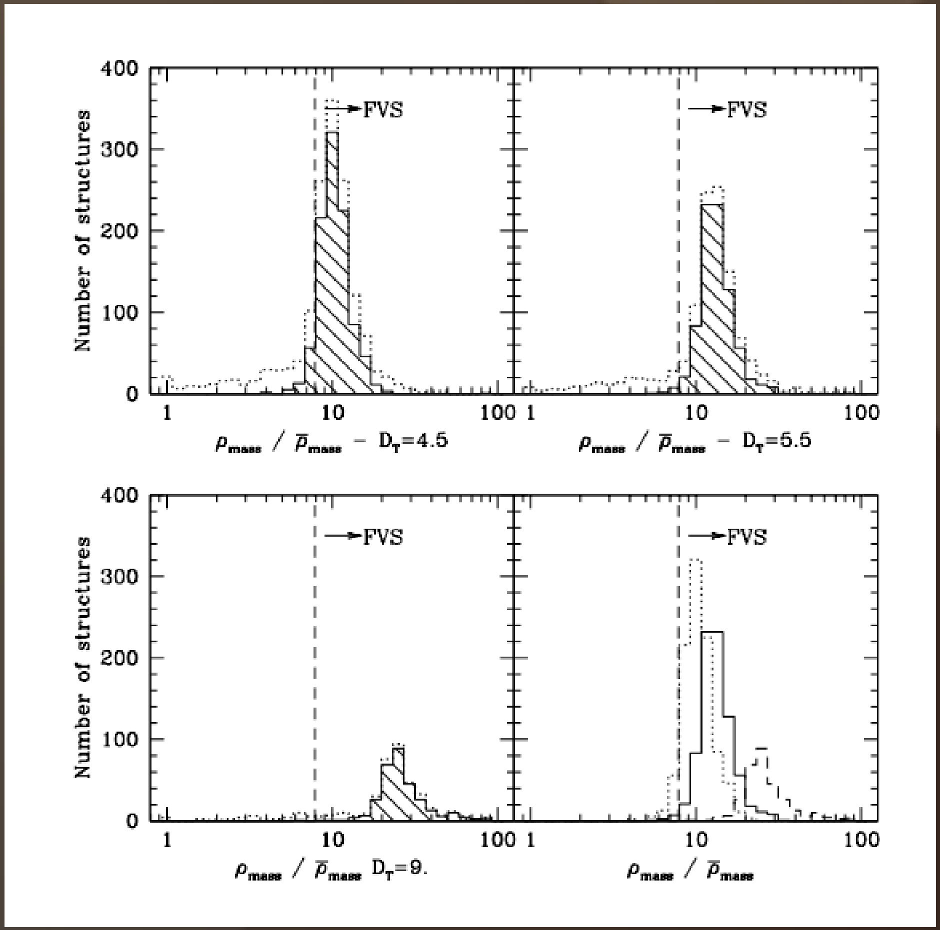

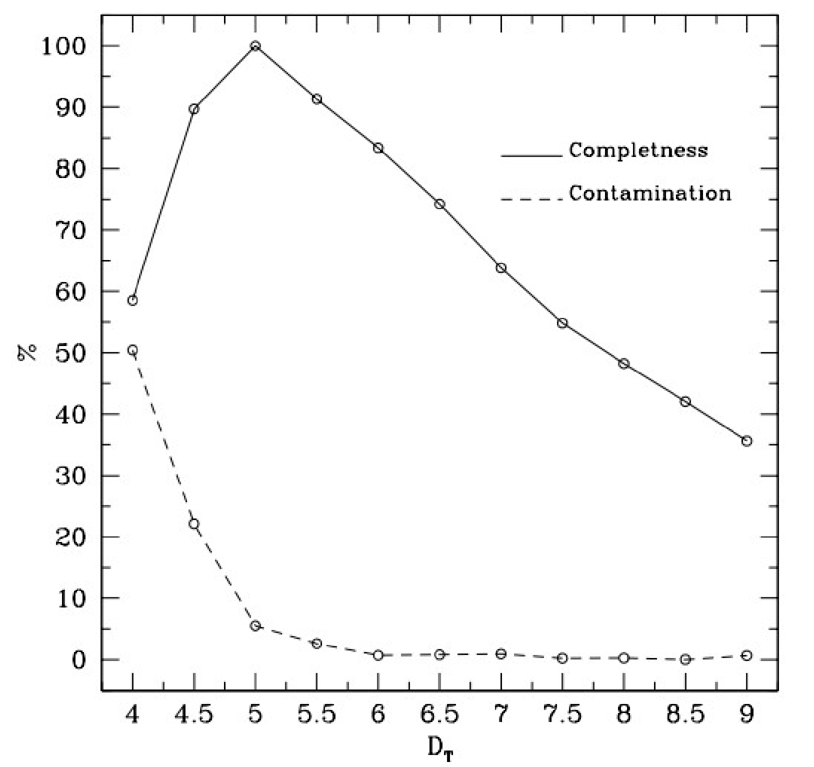

Figure 3. Completeness and contamination of the FVS catalogue as a function of D_T. The chosen value of $D_T = 5.5$ for the compilation of the catalogue of FVS shows the best balance between low contamination and high completeness.

Calibration with LCDM simulations

$$\frac{\bar{\rho}^{mass}_{shell}}{\bar{\rho}^{mass}_{bck}} = 7.88$$

-->

r-band luminosity overdensity = 5.5

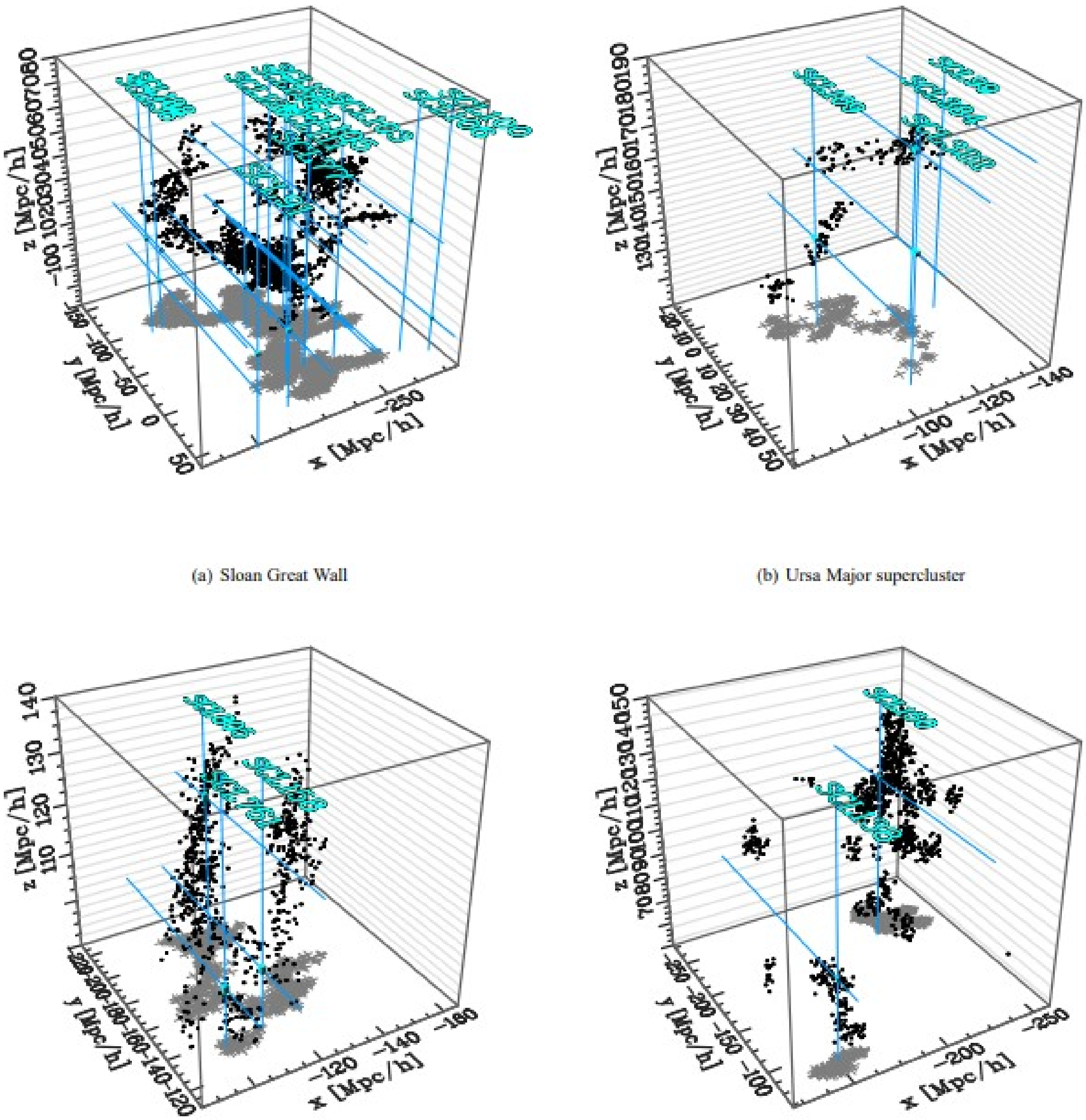

(a) Sloan Great Wall

(b) Ursa Major supercluster

(c) Corona Borealis supercluster

(d) Bootes supercluster

Figure 8. Spatial distributions of galaxies within Future Virialized Systems associated to known superclusters (filled circles). The positions are shown in a cartesian system associated to the equatorial coordinate system (x-axis pointing to the vernal point γ and z-axis pointing to north equatorial pole); the line indicates the observer direction. We also show the centres of superclusters in the catalogues of Einasto et al. (2001), Einasto et al. (2007) and Einasto et al. (2006). Galaxies within nearby FVS are indicated with black dots. In the Sloan Great Wall region (a), we identify a single FVS associated with SCL111, SCL126 and SCL136, indicating that these superclusters may evolve into a single virialized system. The Ursa Major Supercluster, in (b), consists in three large filaments (Kopylova & Kopylov 2006). However, we find a different FVS associated to each filament, suggesting that the filaments would evolve into separate structures. In (c), the Corona Borealis Supercluster SCL158, is part of a larger FVS, that also includes SCL805 and SCL761. So, these three systems could merge to form a single virialized structure in the future. Bootes and BootesA Superclusters in (d) have one-to-one correspondence with FVS, so each system would evolve into a future virialized structure.

Application of the FVS scenario to the real universe.

Adopting a mass-to-luminosity conversion

In the distant future some well known superstructures survive, others merge, and others disperse.

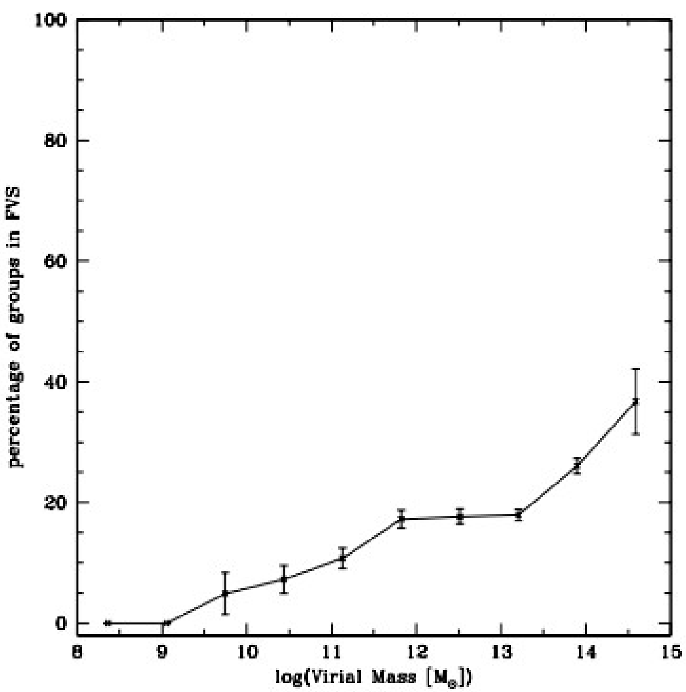

Figure 9. Percentage of DR7 galaxy groups inside FVS with respect to the total number of groups into virial mass bins. The first and second mass bins comprise 21 galaxy groups, although none of them are located into a Future Virialized Structure.

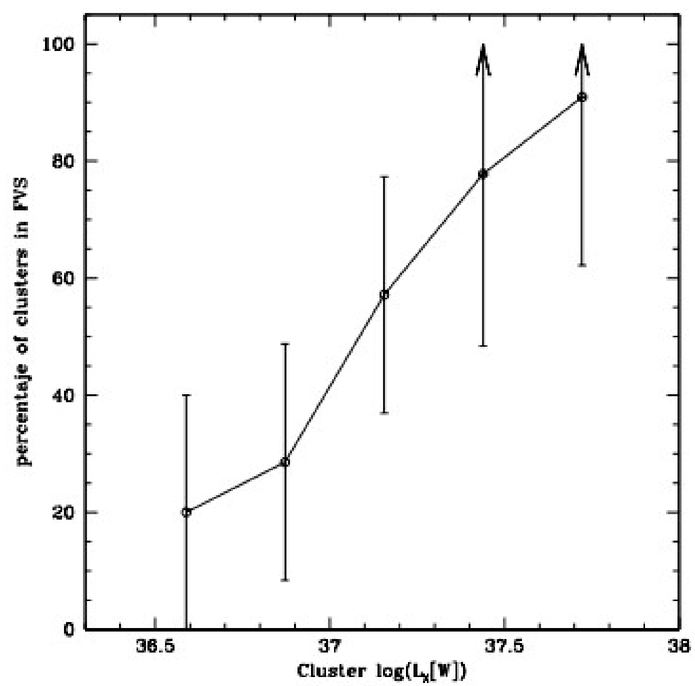

Figure 10. Percentage of X–ray clusters in FVS with respect to the total number of X–ray clusters, as a function of X–ray luminosity.

The majority of massive clusters reside in FVS.

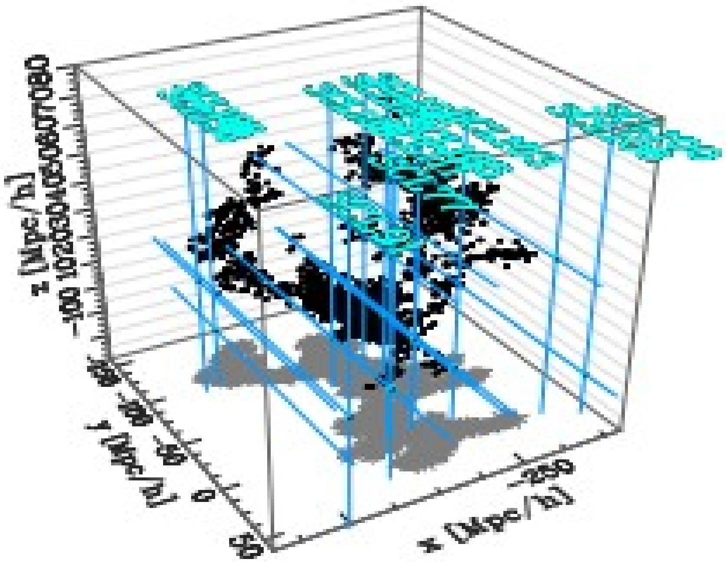

(a) Sloan Great Wall

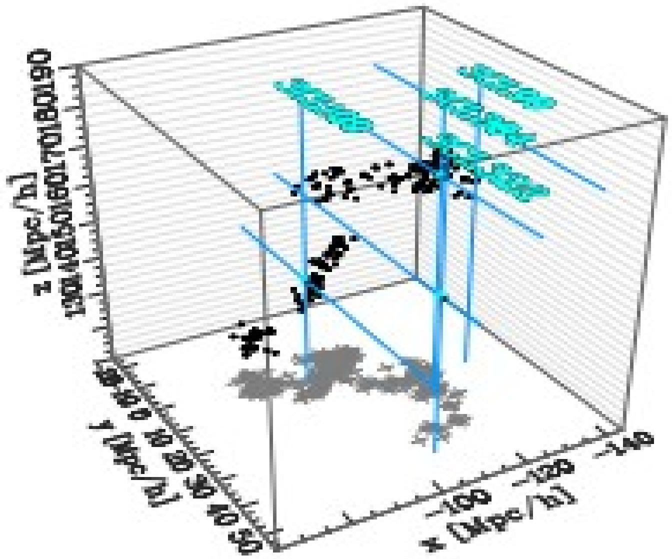

(b) Ursa Major supercluster

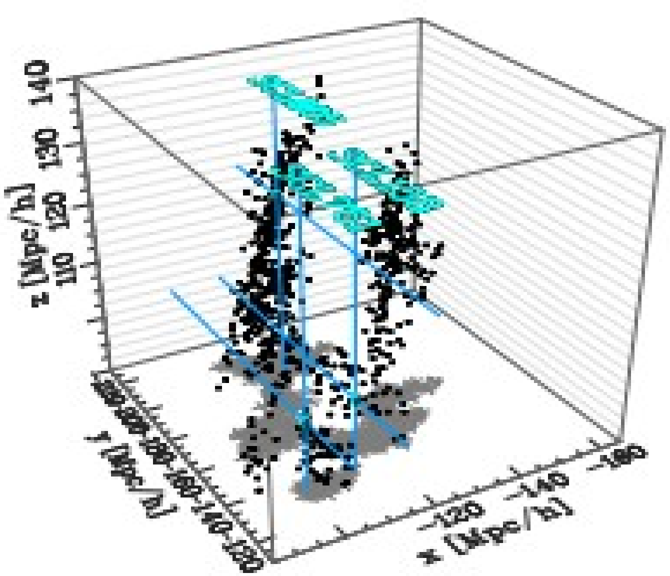

(c) Corona Borealis supercluster

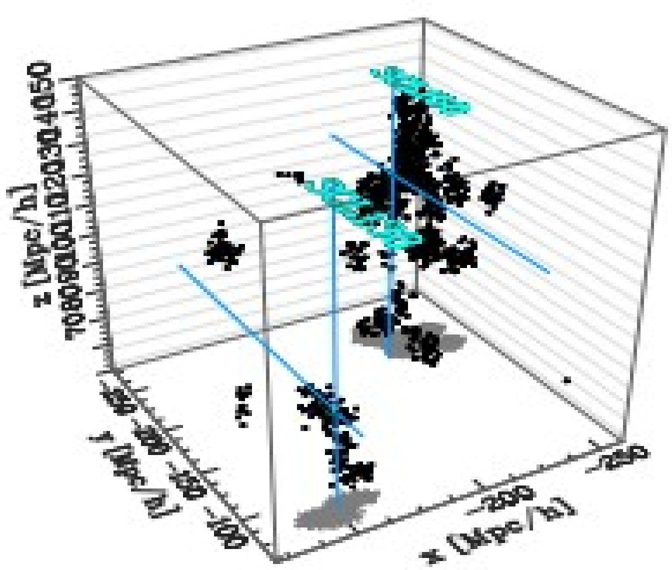

(d) Bootes supercluster

Simulations at large scales

At resolution of few Mpc, gas dynamics and stelar feedback process may be ignored:

- Dark matter only
- Semianalytic model

  - Constrained to reproduce main statistical properties

Can we simulate our local Universe ?

Not just in the statistical sense, but with specific initial conditions that can reproduce observations

Sibelius Dark, Mac. Alpine et al. 2022

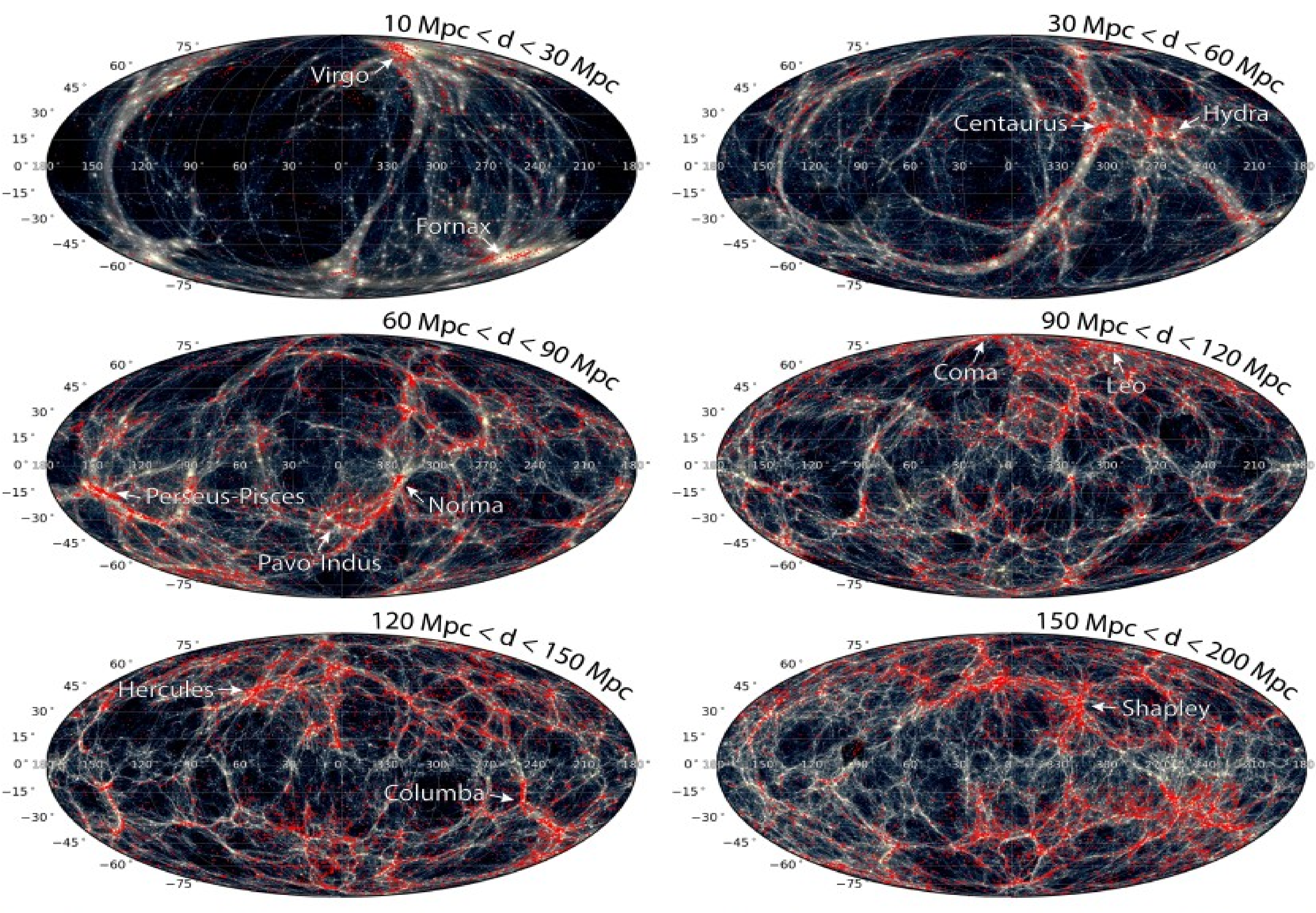

Figure 1. The dark matter distribution of the entire SIBELIUS-DARK volume ($d_{\rm MW} \leq 200$ Mpc), viewed in six spherical shells centred on the Milky Way (blue/green). Each slice is presented as an all-sky-map in a Mollweide projection using the Galactic coordinate system. Overplotted as red points are the galaxies from the 2M++ galaxy sample (Lavaux & Hudson 2011), demonstrating just how well the non-linear structure of the local volume has been encapsulated in the BORG reconstruction. The locations of twelve famous clusters/concentrations are also highlighted.

- Simulating accurately the local volume can lead to more stringent constraints on the cosmological model
- Very reasonable agreement with the observations although:

  There are 4 clusters with log(M) >15, instead of 1 according to LCDM

  Overall scale underdensity of ~5%

Obrigado !

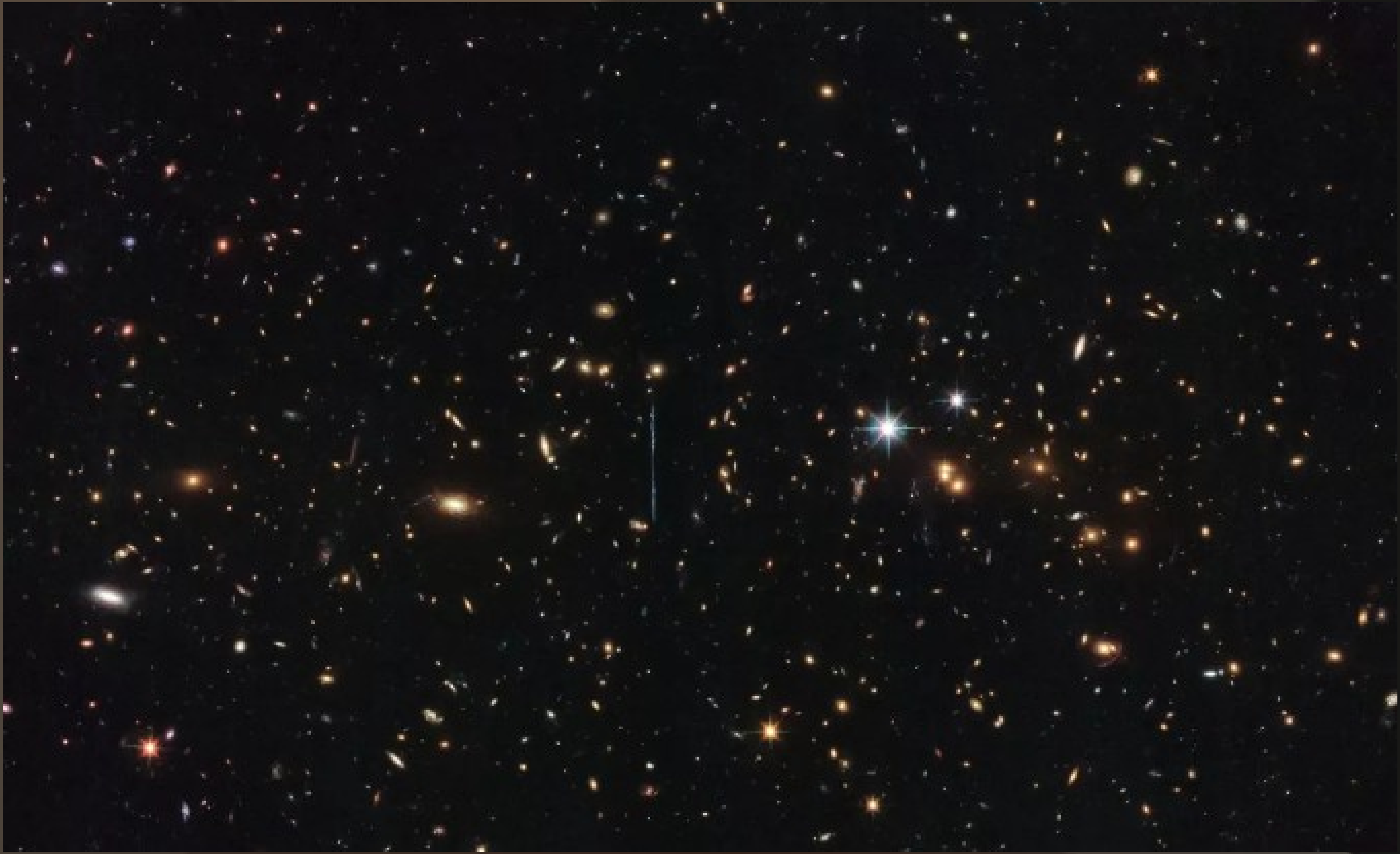

El Gordo cluster, HST image